Local Shell-side Heat Transfer Coefficients in Baffled Tubular Heat Exchangers

T. W. AMBROSE and J. G. KNUDSEN

Oregon State College, Corvallis, Oregon

An experimental study of local heat transfer coefficients in a baffled tubular heat exchanger for five baffle spacings and two tube spacings ($2\frac{3}{16}$-in.-pitch, four-tube bundle, and $1\frac{1}{4}$-in.-pitch, fourteen-tube bundle) is reported. Shell-side air-flow rate was constant for all runs. The variation of the local heat transfer coefficient around the tubes and along the length of the tubes for each tube spacing and baffle spacing was investigated. Average shell-side heat transfer coefficients were evaluated from local values and were found to agree with average values reported in the literature. These average values varied with the six-tenths power of the mass velocity in the heat exchanger. The average Nusselt number and the pressure drop across the exchanger each increased at about the same rate as the number of baffles was increased from two to ten. The average heat transfer rate decreased with decreased tube spacing. This effect was evident from the local heat transfer coefficients, and it is explained on the basis of the mechanism of flow around tubes. An eddy flow zone was detected between the baffles. Average heat transfer rates in the eddy and cross-flow zones were almost equal and were about 15% below the average rate in the longitudinal-flow zone. The variation of the average heat transfer coefficient along a tube definitely showed the effects of baffles. High coefficients occurred in the baffle holes and in the baffle windows.

Baffled tubular-heat exchangers are widely used where heat transmission by forced convection is desired between two fluids. In heat exchangers, the shell side is generally the most difficult to design, because of the shortage of fundamental information concerning flow patterns and associated heat transfer rates on the shell side of heat exchangers. Research conducted on the shell side of heat exchangers has been directed toward the measurement of average shell-side heat transfer coefficients. Although this type of data is useful in the design of similar heat exchangers, it gives little information as to the actual dynamics of flow in the exchanger shell or the effect of flow on heat transfer rates.

The shell-side heat transfer coefficient is dependent upon the geometry and dimensions of the exchanger, as well as upon the properties of the fluid. Variables which describe the exchanger geometrically are baffle type, baffle spacing, baffle size, tube size, tube spacing, and the various clearances between the parts of the heat exchanger. The most common baffle type is the segmental baffle, the type employed in this investigation. The height of segmental baffles is generally 75% of the inside diameter of the shell (*6*); however, various other segmental baffle cuts have been investigated (*2*). A decrease in baffle spacing causes the local velocities and the number of passes across the tube bank to increase. The effects of tube size and tube spacing are difficult to separate, as the effectiveness of a tube is dependent upon the clearance between tubes. An increase in tube spacing causes an increase in heat transfer rate (*3*). The clearances between various parts of the exchanger significantly affect the heat transfer coefficient. The fluid that flows between the baffles and the shell is ineffective, as it does not touch any heat transfer surfaces. As a result, increasing the baffle to shell clearance causes a decrease in the heat transfer rate (*2*). The other major leakage zone is the clearance between the tubes and baffle. As a result the cross flow will be decreased and the flow through the baffle increased.

The purpose of the present investigation was to determine local shell-side heat transfer coefficients in a baffled tubular heat exchanger. From the local coefficients obtained it was possible to (1) compare average shell-side heat transfer coefficients with literature values, (2) evaluate the effect of baffles, (3) evaluate the effect of tube spacing, (4) detect the various flow zones that exist on the shell-side of a heat exchanger, (5) evaluate the heat transfer rate in these zones, and (6) determine the direction of future research of this nature.

EXPERIMENTAL EQUIPMENT

The major components of the experimental equipment included a model heat exchanger, a sensing probe, a direct-current power source, an emf. metering arrangement, and an air source.

The model shell and tube heat exchanger had an effective length of 45-in. The shell was a 6-in.-O.D. cast Lucite plastic tube. The tube bundle was made up of 1-in. aluminum condenser tubes, steel tie-rods, and plastic baffles and tube sheets. A photograph of the tube bundle is shown in Figure 1. The shell had an entrance and exit so air could be provided to the shell-side. The tube bundle had no provision for handling a tube-side fluid. The baffles were $\frac{1}{8}$-in.-thick plastic sheets. Table 1 shows the dimensions and tolerances of the shell, tubes, and baffles.

TABLE 1. DIMENSIONS OF HEAT EXCHANGER COMPONENTS IN.

Shell	
Inside diameter	5.72 ± 0.03
Outside diameter	5.94 ± 0.03
Inside length	45
Tubes	
Outside diameter	1.000 ± 0.001
Baffles	
Baffle diameter	5.594 ± 0.002
Height at cut	4.290 ± 0.002
Drilled holes	1.063 ± 0.010

A sensing probe was constructed to measure local heat transfer coefficients. An electrically heated resistance ribbon in contact with a cooling fluid assumes a temperature which is related to the heat transfer coefficient, the cooling-fluid temperature, and the power supplied to the ribbon. An energy balance on the ribbon gives an expression relating these variables [Equation (1)].

A drawing of the sensing probe is shown in Figure 2. It was fabricated from a 6-in. piece of 1-in.-O.D. Lucite plastic rod, drilled with a $\frac{1}{8}$-in. hole along its longitudinal axis. A 1-in. section at each end of the tube was machined and threaded. Three 1-in.-wide by 0.002-in.-thick pieces of resistance ribbon were wrapped around the plastic bar as shown in Figure 3. The resistance ribbon used was Tophet *C*, having a resistance of 0.271-ohm/ft. and a thermal conductivity of 7.63-B.t.u./(hr.)(sq. ft.)(°F./ft.). The ribbons were held in place by copper bus bars embedded in the plastic, which also served to supply electric power to the resistance ribbons. Power leads were soldered to the lower connecting bar in such a manner that the three ribbons were in series. The leads were brought into the plastic piece through the holes along its horizontal axis. Seven iron-constantan thermocouples were located in a groove under the center ribbon, as shown in Figure 2. The thermocouple junctions were electrically insulated from the ribbon by a layer of Saran wrap. At the opposite end from the power leads the thermocouple leads entered the probe, which was supported between two pieces of aluminum condenser tubing with plastic adapters threaded to the plastic piece. The thermocouple leads were connected to a multiple-junction selector switch attached to one of the support tubes. A photograph of the sensing probe attached to one support tube is shown in Figure 3. Direct current was supplied by passing alternating current through a voltage stabilizer and a selenium rectifier. The emf.'s of the various thermocouples were measured with a Leeds and Northrup precision potentiometer.

The above-described sensing-probe assem-

T. W. Ambrose is with General Electric Company, Richland, Washington.

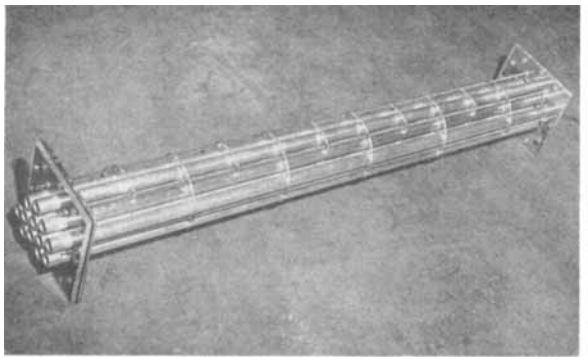

Fig. 1. Assembled tube bundle.

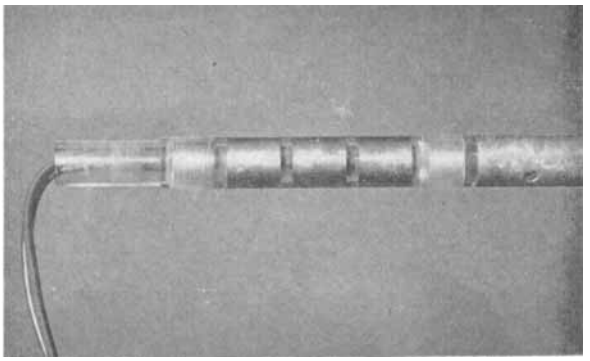

Fig. 3. Sensing probe attached to one support tube.

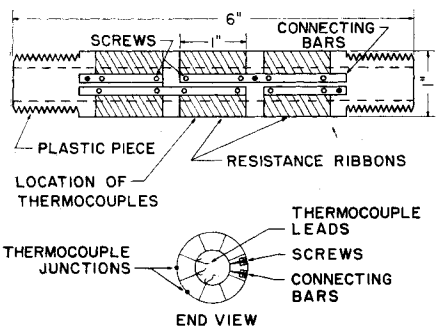

Fig. 2. Detail of sensing probe.

bly could replace any of the aluminum condenser tubes in the bundle or could be located at any given point along the length of the exchanger. In this manner, it was possible to determine local heat transfer coefficients at any location in the tube bundle.

The shell-side fluid was air supplied by a Roots-type blower rated at 280 cu. ft./min. at 3½ lb./sq. in. gauge. The air from the blower passed through a 2-in. pipe to the coolers and then to the model heat exchanger. Sharp-edged orifices equipped with manometers were used to determine the air flow rate, and the pressure drop across the exchanger was measured with a manometer. The air temperature was measured by a thermocouple located in the heat exchanger outlet. A schematic drawing of the air flow system is shown in Figure 4.

EXPERIMENTAL DATA

Five baffle spacings and two tube spacings were investigated. Original data are available (*1*). The air flow rate was maintained constant at 60 cu. ft./min. (60°F., 1 atm.) throughout the study. Shell-side air temperature was usually quite close to room temperature. In all, about 7,000 local heat transfer coefficients were obtained. The data are summarized briefly in Table 2.

Various baffle spacings were studied by varying the number of baffles in the exchanger; zero, two, four, six, and ten baffles equally spaced in the 45-in. shell. The number of positions investigated along each tube for the five baffle spacings was limited to the locations shown to scale in Figure 5. (Reference should be made to Figure 5 in subsequent discussions regarding locations in the heat exchanger.) These locations are at the inlet, outlet, and center of the model heat exchanger, as well as in each baffle hole and 2 in. on each side of the baffle. In the four- and six-baffle cases, the region downstream from the center line of the exchanger was not investigated, as it was assumed to be symmetrical with the upstream region. The same reasoning was used in the ten-baffle case, where only the first three spaces were studied.

One-inch outside-diameter tubes in two triangular pitches: a $2\frac{3}{16}$-in. tube pitch, which comprised a four-tube bundle, and a $1\frac{1}{4}$-in. tube pitch, which comprised a fourteen-tube bundle. As may be seen in Figure 6, the tube spacing of the four-tube bundle is identical with that of the same four tubes in the fourteen-tube bundle. The tube and thermocouple numbering system is also shown in Figure 6.

CALCULATION OF THE LOCAL HEAT TRANSFER COEFFICIENT

To calculate local heat transfer coefficients, required data were the current

Table 2. Summary of Experimental Data

No. of baffles	No. of positions studied along tube	Total No. of local coefficients measured	Air flow rate, cu. ft./min. cfm (60°F., 1 atm.)
	Four-tube bundle		
0	7	196	59.5
2	11	308	59.1
4	10	280	59.5
6	12	336	59.5
10	9	252	59.1
	Fourteen-tube bundle		
0	7	686	59.3
2	11	1,078	59.1
4	10	980	59.3
6	12	1,176	59.4
10	9	882	59.4

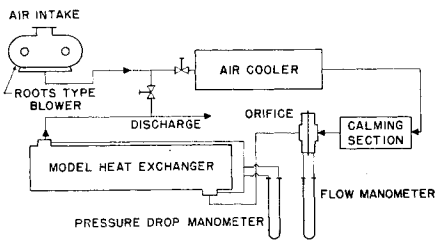

Fig. 4. Air flow system.

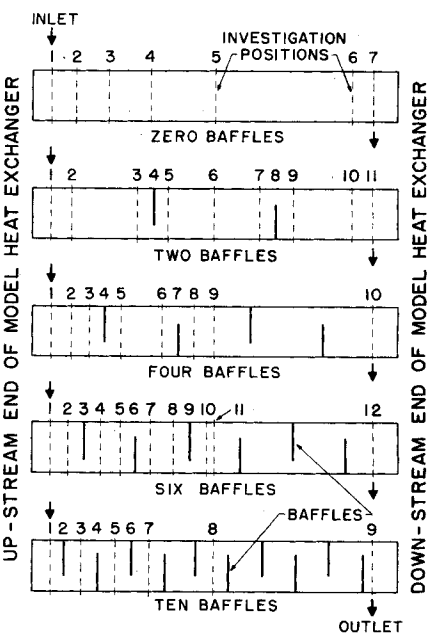

Fig. 5. Baffle spacings and positions investigated.

in the resistance ribbon and the millivolt readings from the seven sensing-probe thermocouples and the air thermocouple.

A general expression for the local heat transfer coefficient is developed by making an energy balance around a differential length of resistance ribbon. The following equation results, as shown by Giedt (*5*):

$$h = \frac{\frac{i^2R}{W} + \frac{kZ}{Wr^2}\frac{d^2t}{d\theta^2} - \frac{q_{rad}}{A} - \frac{q_{cond}}{A}}{t - t_a} \quad (1)$$

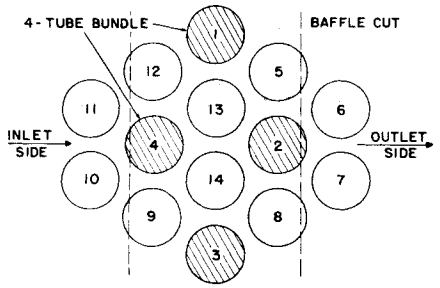

Fig. 6a. Tube arrangements numbered at up-stream end of exchanger.

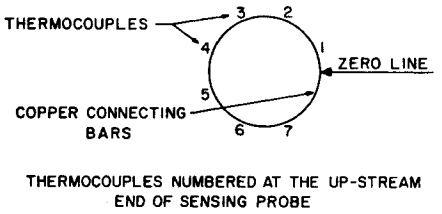

Fig. 6b. Thermocouple numbering system.

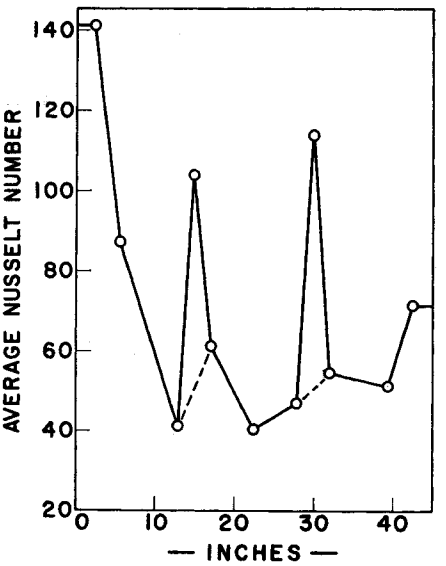

Fig. 7. Plot for determination of average Nusselt number for model heat exchanger
———— high Nusselt number
---------- low Nusselt number

The radiation term was neglected in calculating the local heat transfer coefficients, it being assumed to be negligible in the majority of cases. This assumption is in agreement with other investigators who have used this method (*3*, *4*). The rate of conduction of heat into the plastic probe was also assumed to have a negligible effect on the local heat transfer coefficient. This assumption was justified by a maximizing type of calculation (*1*). Neglecting the radiation and conduction term and substituting in the numerical constants, one can write Equation (1) as

$$h = \frac{11.10i^2 + 2404(d^2t/d\theta^2)}{t - t_a} \qquad (2)$$

Equation (2) was used to calculate the local heat transfer coefficients. The second derivative was evaluated with a Milne three-point method (*9*). The actual calculation of the local heat transfer coefficients was performed on a digital computer. An average heat transfer coefficient was evaluated at each position from the arithmetic average of the seven local coefficients around the circumference of the tube. A Nusselt number for each position was calculated by means of this average heat transfer coefficient.

EXPERIMENTAL RESULTS

Average Shell-side Nusselt Numbers

The average shell-side heat transfer rates for the heat exchanger were determined and compared with those of Williams and Katz (*13*) and Donohue (*2*). Two values of the average Nusselt number were calculated. In each, the average Nusselt number at each cross section (including all tubes) was plotted vs. exchanger length as shown in Figure 7. The high average Nusselt number for the heat exchanger was obtained by integrating the plot in Figure 7 and dividing by the heat-exchanger length. At each baffle a maximum in the Nusselt number is observed. The low average Nusselt number was obtained by neglecting these high peaks, as shown by the broken lines. The difference between the high and low average Nusselt numbers indicates the effect of the high heat transfer coefficients at the baffle holes. The effect could be obtained more accurately by a detailed study of local coefficients in the vicinity of the baffle.

The term $(hd/k)(C_p\mu/k)^{-1/3}$ was calculated from the average Nusselt number and the Prandtl number of air, which was taken as 0.7 in all cases. In Figure 8 the term $(hd/k)(C_p\mu/k)^{-1/3}$ is plotted against the weighted Reynolds number (dG_e/μ). Also plotted are two curves from Williams and Katz (*13*). The two remaining curves were obtained by Donohue (*2*) on the basis of data of Short (*11*). All the curves shown in Figure 8 are for segmental baffled heat exchangers with triangular tube pitches.

The curves representing the high values of average Nusselt numbers are above those of the other workers. However, a straight line with a 0.6 slope is obtained. The curves representing the low average heat transfer coefficients lie very close to the data of Williams and Katz, particularly for the fourteen-tube case, which is most nearly like the exchangers studied by these investigators. The slope of the curve, however, is less than 0.6.

The method used to evaluate the high Nusselt numbers was thought to overweight the heat transfer coefficients at the baffles. It is believed, however, that the high average values are closer to the true average than the low average values. The contribution of the high heat transfer coefficients at the baffles is greater for the ten-baffle case than for the two-baffle case. This is apparent when the low average values are compared with the high average values. For the two-baffle case the difference between the two average Nusselt numbers is about 5%, and for the ten-baffle case about 25%. This also accounts for the curve representing the low values having a slope of less than 0.6. The true curve is thought to pass between the high and low points for the two-baffle case and to have a 0.6 slope.

The results in Figure 8 show good agreement of the present work with that of other investigators. These results are always somewhat high, but this is expected because of the large tube size used. All other investigators have studied tube diameters no greater than ¾-in., while the present results are based on a 1-in.–O.D. tube.

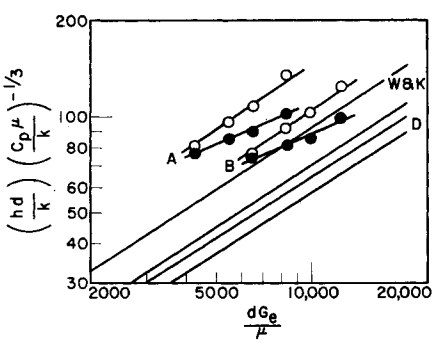

Fig. 8. Correlation of shell-side heat transfer data, ○ high values, ● low values

Curve		
A	Ambrose & Knudsen	(6″ shell, 1″ tubes, 2-3/16″ tube pitch)
B	Ambrose & Knudsen	(6″ shell, 1″ tubes, 1-1/4″ tube pitch)
W & K	Williams & Katz	(6″ shell, 5/8″ tubes, 3/4″ tube pitch)
	Williams & Katz	(8″ shell, 1/2″ tubes, 5/8″ tube pitch)
D	Donohue	(8″ shell, 5/8″ tubes, 3/4″ tube pitch)
	Donohue	(6″ shell, 5/8″ tubes, 7/8″ tube pitch)

Effect of Baffles

The addition of baffles to the tube bundle increased the shell-side heat transfer rate. This effect is shown in Figures 8 and 9. In Figure 9 average shell-side Nusselt numbers for the four- and fourteen-tube cases are plotted against the number of baffles. The curve for the four-tube bundle is always higher than that for the fourteen-tube bundle with the exception of the no-baffle case. This reversal at the no-baffle case was expected, since the mass flow rate was increased by the addition of tubes. After the addition of two baffles, the rate of increase in the Nusselt number by adding baffles is nearly the same for both four- and fourteen-tube cases.

The addition of baffles to the tube bundle increased the pressure drop across the shell-side of the heat exchanger. Figure 10 shows a plot of the pressure drop (inches of water) vs. the number of baffles present. The points lie very nearly on a straight line with similar slopes for both the four- and fourteen-tube bundles. It can be seen from Figures 9 and 10 that increasing the number of baffles from two to ten increases the heat transfer rate and the pressure drop. The rate of increase of each is about the same as the number of baffles is increased.

Effect of Tube Spacing

As shown in Figure 9, the 2 $\frac{3}{16}$-in. pitch arrangement had a higher heat transfer rate than the 1¼-in. pitch for all baffle cases, despite the fact that velocities are higher in the latter case. The tube area for the smaller pitch was only 93.5 to 95.5% as effective as that for the greater tube pitch. This effect was noted in Short's (*11*) data, which show that, for a heat exchanger with ⅜-in. tubes on a ½-in. triangular tube pitch, the area was from 92.9 to 93.8% as effective as when the tubes were spaced on a $1\frac{1}{16}$-in. tube pitch for three, seven, eleven, fifteen and nineteen baffles.

When the tube pitch was decreased by the addition of tubes, the clearances between the tubes were greatly decreased (Figures 6 and 11). The decreased flow area caused an increase in local velocities throughout the heat exchanger. Generally, increased heat transfer rates are associated with increases in the local mass velocities; however, in the results cited above, just the reverse was true for the average heat transfer coefficients.

A comparison of the four tubes, which had the same location in each tube arrangement, indicated that tubes in the four-tube bundle always had higher local heat transfer coefficients than the same tubes in the fourteen-tube bundle. This effect is explained by examining the characteristics of the flow past the tubes. When only the four tubes were in the shell, as in Figure 11*A*, the area behind the lead tube was characterized by a turbulent wake almost as wide as the tube and

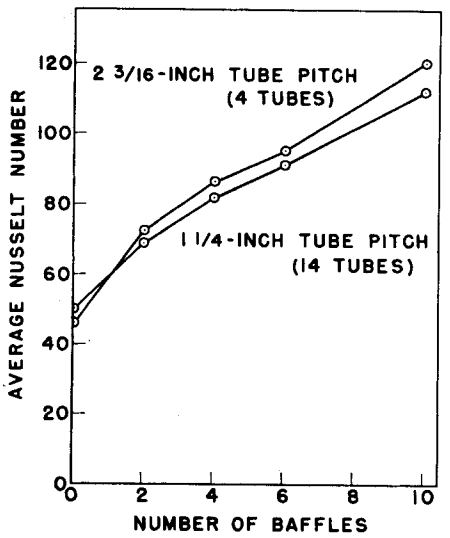

Fig. 9. Effect of baffles on the heat transfer rate.

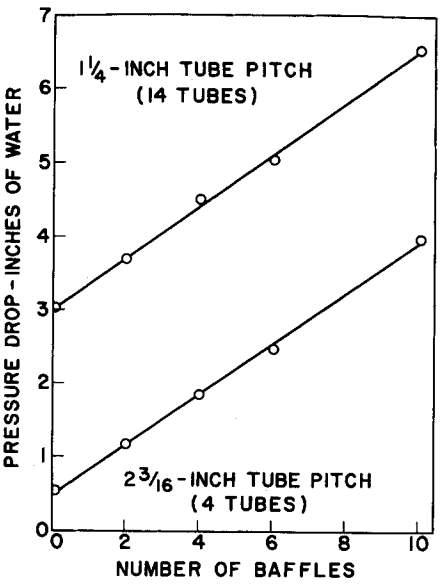

Fig. 10. Effect of baffles on pressure drop.

probably extending to the next tube (*12*). This turbulent wake has the effect of producing a high heat transfer coefficient on the trailing tube. Although the local velocity of the stream was lower when compared with the fourteen-tube bundles, the turbulence caused higher local coefficients. The fluid leaving the trailing tube had to flow around the baffle cut before striking the lead tube in the next baffle space. This fluid was also in a highly turbulent state, and the local coefficients on the lead tube were even higher than those on the trailing tube.

With fourteen tubes there were two lead tubes instead of one, as shown in Figure 11*B*. All tubes were located quite close to each other. Owing to the close spacing of the tubes, the turbulent wake was confined to a narrow region behind the tubes and did not extend to the

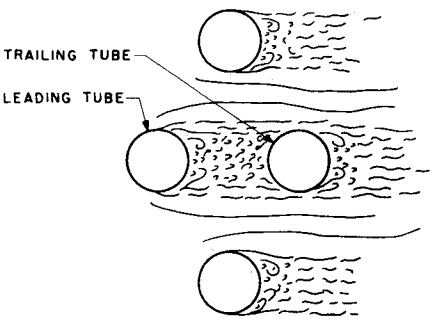

Fig. 11*a*. Flow pattern across tube bank (four tube bundle).

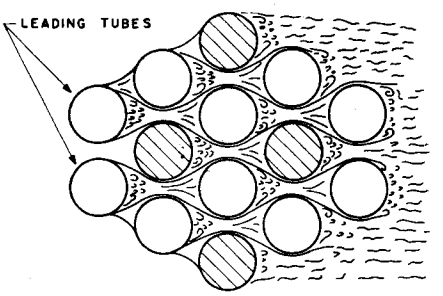

Fig. 11*b*. Flow pattern across tube bank (fourteen tube bundle).

downstream tube (*12*). This is illustrated in Figure 11*B*. For this reason, local heat transfer coefficients are lower than in the four-tube case.

The local heat transfer coefficients for each position were plotted vs. the angle θ, measured counterclockwise around the tube when the sensing probe was observed from the upstream end. The 0-deg. point was arbitrarily set on the outlet side of the exchanger, as shown in Figure 6. Thermocouple 1 was located at 22½ deg. from the zero point and a thermocouple located every 45 deg. thereafter until thermocouple 7 was reached at 292½ deg. from the zero point. The position at 337½ deg. was the region occupied by the connecting bars.

Parts *A* and *B* of Figure 12 show a comparison of the local heat transfer coefficients at position 3 for tubes 2 and 4 for the four- and fourteen-tube bundles and the ten-baffle case. The lead tube in the four-tube case (tube 2) was noted to have a greater heat transfer rate at $\theta = 0$ deg. when compared with the trailing tube (tube 4), owing to high turbulence in the fluid coming around the baffle. At $\theta = 180$ deg. the heat transfer rates for the lead tube were slightly lower than those of the trailing tube. For both tubes 2 and 4, the heat transfer coefficients for the fourteen-tube case were considerably less than for the four-tube case. This is consistent with the explanation outlined above.

Flow Zones

Gupta and Katz (*7*) visually detected two flow zones in the space between

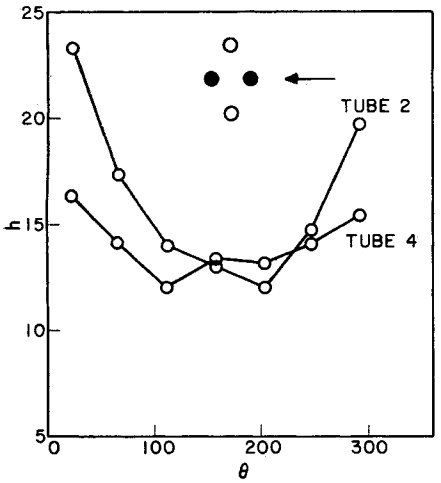

Fig. 12*a*. Local heat transfer coefficients for position 3 in exchanger with 10 baffles and 4 tubes.

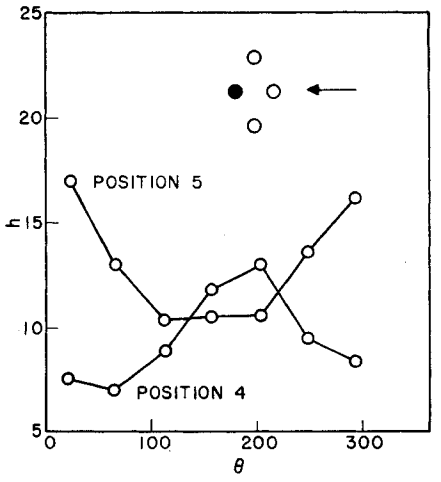

Fig. 13*a*. Local heat transfer coefficients for tube 4 in exchanger with 6 baffles and 4 tubes.

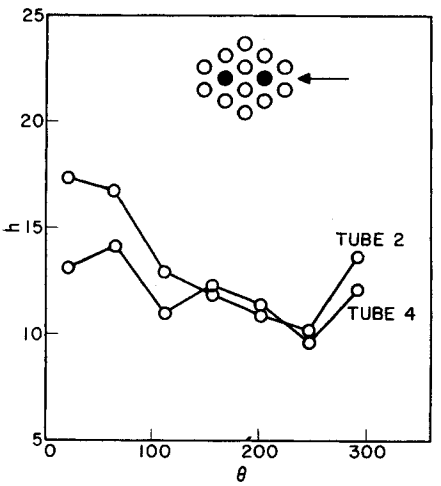

Fig. 12*b*. Local heat transfer coefficients for position 3 in exchanger with 10 baffles and 14 tubes.

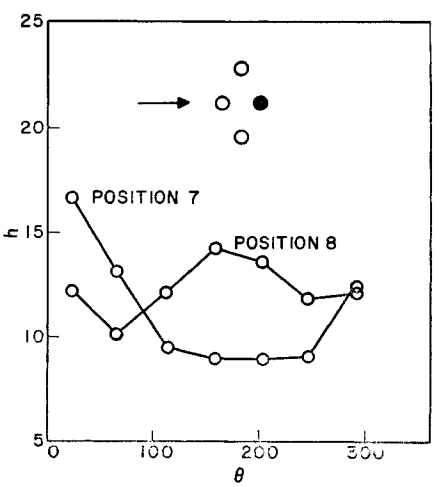

Fig. 13*b*. Local heat transfer coefficients for for tube 2 in exchanger with 6 baffles and 4 tubes.

baffles: an eddy zone located behind a baffle and a cross-flow zone located in the region in front of the next baffle. These observations were made in a glass heat exchanger which had no clearance between tubes and baffles or between baffles and shell. Eddy zones were shown by Gunter, Sennstrom, and Kopp (*6*) to exist behind solid baffles.

In both these investigations no leakage occurred through the baffle, and the eddy zone was not disturbed by flow through or around the baffle, nor was the effect of leakage on the eddy zone determined. From the present investigation, sufficient data were available for the regions between baffles to permit the detection of the eddy zones and the determination of the heat transfer rates in these localities.

In the case of the fourteen-tube bundle, the eddy zone was present but was not so pronounced as in the four-tube case.

Evidence of the eddy zone is shown by the local heat transfer coefficients. In the four-tube bundle, positions 5 and 8 were located in the cross-flow zone and were used as a basis of comparison. Figure 13*A* shows that at position number 5 the local heat transfer coefficient for tube 4 has a definite maximum near $\theta = 0$. For position 4 the local heat transfer coefficient for tube 4 has a minimum in the region of $\theta = 0$. The complete reversal of these two curves indicated that the fluid was approaching tube 4 in a different direction at position 5 than at position 4. This can be explained if position 4 lies in an eddy zone. This same effect is shown in Figure 13*B* for the region between baffles 2 and 3. Here the trailing tube is tube 2. Tubes 1 and 3 show this same reverse type of curve for position 4 as compared with position 5 and for position 7 as compared with position 8. Thus the eddy zone was large enough to cover the entire bundle at the downstream side behind the baffle. For the fourteen-tube, six-baffle case, the data for position 7 and tubes 1 to 5 and 8, 9, 12, 13, and 14 indicated that tubes 2, 5, and 8 showed evidences of the eddy zone; tubes 4, 9, and 12 had the normal type of curve, that is, the high coefficients near the leading edge; tubes 1 and 3 showed evidences of the eddy zone; and tubes 13 and 14 indicated neither a maximum nor minimum, yielding heat transfer rates which were nearly the same completely around the tube.

Evidence of the eddy zones was noted at positions 2 in. behind the baffles in both the two- and four-baffle spacings; however, insufficient data prevented detailed examination of the eddy zones. In the ten-baffle arrangement a single examination point was located midway between baffles (2 in. on each side of the baffles). No evidence of an eddy zone was noted at any of the tubes in either the four- or fourteen-tube bundles. A study of more locations between the baffles would allow a more thorough analysis.

Heat Transfer Rates in Various Zones

The heat transfer rates in the longitudinal flow zone, the cross-flow zone, and the eddy zone were compared for the fourteen-tube case and six-baffle arrangement. The longitudinal flow zone between baffles 1 and 3 through the window of baffle 2 had an average heat transfer coefficient of 13.93 B.t.u./(hr.) (sq. ft.) (°F.). The longitudinal-flow zone was considered as the region enclosed by the shell between baffles 1 and 3 and two imaginary planes extending from the cut of baffle 2 to the base of baffles 1 and 3 respectively. The average heat transfer coefficients of the cross-flow and of the eddy zones were taken as the average of the local coefficients on the transverse section through these zones. The average heat transfer coefficients in the cross-flow zones at positions 5 and 8 were 11.61 and 11.36 respectively. The average heat transfer coefficients in the eddy zones at positions 4 and 7 were 11.01 and 11.57. The average coefficients of the two zones do not seem to be significantly different when compared on the basis of the variation between cross-flow and eddy zones. The average of these four values is 11.40, which is about 18% lower than the value for longitudinal flow. Insufficient data were taken for the two, four, and ten baffles for a comparison of the heat transfer rates in various zones.

Heat Transfer Rates Along the Length of the Heat Exchanger

The heat transfer coefficients along the length of the heat exchanger varied considerably. To show this variation, the average Nusselt numbers at each position on a tube were plotted vs. distance from the upstream end of the exchanger. Figure 14 shows the distribution of the average Nusselt number at each position along tube 10 for the fourteen-tube bundle.

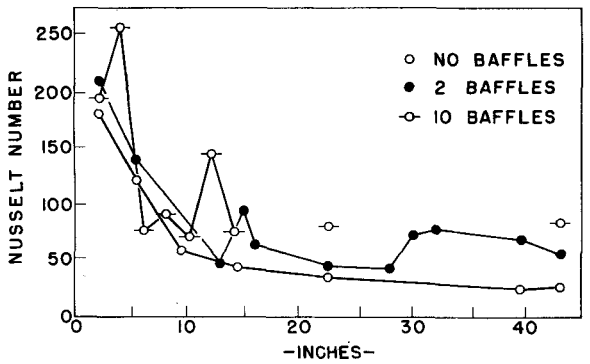

Fig. 14. Average local Nusselt numbers along tube 10.

High Nusselt numbers were observed at the entrance, and these showed small variation with the number of baffles in the exchanger. With no baffles present, the Nusselt number decreased rapidly with length and became constant after the midpoint of the exchanger. The constant value was about one sixth of the value at the entrance.

For the two-baffle case, the Nusselt number decreases with length, then increases to a maximum where the tube goes through the first baffle. The Nusselt number then decreases and increases again to a maximum at the point in the baffle window where the tube passes the baffle. Similar phenomena are observed for all baffle spacings. A large increase is noted in the Nusselt number as the tube passes through the hole in the baffle. These results indicate semiquantitatively that a small clearance between the tube and baffle has the effect of producing a high Nusselt number at this point. The baffle also affects the tube in the baffle window in that a moderate increase occurs in the Nusselt number at the point in the baffle window where the tube passes the baffle.

Heat Transfer Rates Around a Single Tube

True cross flow through the tube bundle was most nearly obtained in the region between baffles in the ten-baffle case. At points midway between the baffles, the lead tubes all showed similar circumferential variation of the local heat transfer coefficients. This pattern is characterized by a high heat transfer coefficient at the leading edge of the tube. The local coefficient decreased with increasing distance away from the leading edge until a minimum was reached near the trailing edge of the tube. The trailing tube in the bundle had a lower heat transfer coefficient at the leading edge when compared with the lead tube, but it had a higher coefficient on the trailing side of the tube than did the lead tube. About a twofold decrease in heat transfer rate around tubes in cross flow was observed. The variation around the tubes in the bundle was considerably different from that observed on a single cylinder in cross flow.

CONCLUSIONS

Local heat transfer coefficients were determined on the shell side of a baffled tubular heat exchanger. Baffle spacing and tube spacing were varied, but volumetric flow rate was held constant. An average Nusselt number for the shell side was calculated from these local coefficients, both including and neglecting the high values at the baffles. It is believed that the average Nusselt number which includes the high value at the baffles is closer to the true Nusselt number. These average values calculated from the measured local coefficients agree fairly well with those of other investigators.

Addition of baffles caused an increase in the average Nusselt number and the pressure drop at a constant flow rate. The average Nusselt number and the pressure drop across the exchanger each increased at about the same rate as the number of baffles was increased from two to ten.

Increasing the tube spacing from $1\frac{1}{4}$ to $2\ \frac{3}{16}$ in. at constant flow rate increased the average heat transfer coefficient for all baffle arrangements except the zero-baffle case.

Between baffles a cross-flow and eddy zone were detected from the variation of local coefficients on the tubes. The eddy zone was detected for all but the ten-baffle case, for which insufficient data were available. For the fourteen-tube, six-baffle case there was little difference in the average rate of heat transfer in the longitudinal-flow, cross-flow, and eddy-flow zones.

The variation of average heat transfer coefficient along a tube definitely showed the effect of baffles in a heat exchanger. Large values are obtained in baffle holes, and moderately large values occur in the baffle window where the tube passes the baffles.

ACKNOWLEDGMENT

Appreciation is expressed to the National Science Foundation for a grant to support the research described here.

NOTATION

A = area, sq. ft.; A_c, cross flow area in tube bank; A_w, baffle window area
C_p = specific heat at a constant pressure, B.t.u./(lb.)(°F.)
d = diameter of tube, ft.
G_e = weighted mass velocity, lb./(hr.)(sq. ft.) = $w/\sqrt{A_w A_c}$
h = heat transfer coefficient, B.t.u./(hr.)(sq. ft.)(°F.)
i = current, amp.
k = thermal conductivity, B.t.u./(hr.)(sq. ft.)(°F.)/ft.
$q_{cond.}$ = heat conducted into plastic specimen, B.t.u./hr.
$q_{rad.}$ = heat radiated from ribbons, B.t.u./hr.
R = resistance of ribbon, ohms/ft.
r = radius, ft.
t = temperature, °F.; t_a, air temperature
W = width of resistance ribbon, ft.
w = mass flow rate, lb./hr.
z = thickness of resistance ribbon, ft.

Greek Letters

θ = angle measured from leading edge of a tube, deg.
μ = viscosity, lb./(ft.)(hr.)

LITERATURE CITED

1. Ambrose, Tommy W., Ph.D. thesis, Oregon State Coll., Corvallis (1957), available from University Microfilms, Ann Arbor, Mich.
2. Donohue, Daniel A., *Ind. Eng. Chem.*, **41**, 2499 (1949).
3. Drake, R. M., Jr., *J. Appl. Mechanics*, **16**, 3 (March 1949).
4. ———, et al., Am. Soc. Mech. Engrs. paper 52-A-59 (1952)
5. Giedt, W. H., *Trans. Am. Soc. Mech. Engrs.*, **71**, 375 (1949).
6. Gunter, A. Y., H. R. Sennstrom, and S. Kopp, paper presented at the annual meeting of the Am. Soc. Mech. Engrs., Atlantic City, N. J., (December, 1947).
7. Gupta, Rajeshwar, K., and Donald L. Katz, *Ind. Eng. Chem.*, **49**, 998 (1957).
8. Kern, Donald Q., "Process Heat Transfer," p. 130, McGraw-Hill Book Company, Inc., New York (1950).
9. Milne, William E., "Numerical Calculus," p. 96, Princeton Univ. Press (1949).
10. Short, B. E., *Trans. Am. Soc. Mech. Engrs.*, **64**, 780 (1942).
11. ———, *Univ. Texas Publ.* 4324, pp. 1–55 (1943).
12. Wallis, R. P., *Engineering*, **148**, 423 (1934).
13. Williams, Richard B., and Donald L. Katz, *Trans. Am. Soc. Mech. Engrs.*, **74**, 1307 (1952).

Manuscript received Aug. 12, 1957; revised Dec. 10, 1957; accepted Jan. 13, 1958.